Hot deformation studies on 2.7% Si steel using gleeble thermo-mechanical simulator

KUMAR ANIKET ANAND*, KARTIK NAGESWARAN,
VINOD KUMAR and ATUL SAXENA
R&D Centre for Iron & Steel, Steel Authority of India Ltd.,
Ranchi, Jharkhand-834 002, India

Abstract : Uni-axial hot compression tests were conducted at different temperatures (1173-1423 K) and at strain rates of 0.1, 1, 10 and 100/s using Thermo-mechanical Simulator (Gleeble-350^{0}C System) on a 2.7% Si electrical steel to understand the hot workability issues associated with this steel during hot rolling. The flow curves obtained revealed dynamic recovery as the predominant softening mechanism at majority of hot deformation conditions except at lower temperature and high strain rate where work hardening was observed. However, the work hardening was not very prominent due to ferrite structure throughout the hot deformation temperature range established by Thermo-Calc software. Small amount of cementite (pearlite) transformed from austenite along prior ferrite grain was observed due to presence of carbon in excess of 0.02. Strain rate sensitivity varied within a narrow range of 0.18 - 0.21 with rising tendency with an increase in temperature.

Keywords : Silicon steel, Electrical steel, Hot deformation, Hot rolling.

INTRODUCTION

Electrical steels, also called lamination steel or silicon electrical steel, are an important category of iron-silicon alloys containing 1-5 wt % silicon and very low carbon (less than 0.005 wt %)[1, 2]. Silicon significantly increases the electrical resistivity of the steel, which decreases the induced eddy currents and narrows the hysteresis loop of the material, thus lowering the core loss[3].

Electrical steels contain generally unavoidable Mn and S after the metallurgical process. The Mn and S would even be used as alloy elements in oriented electrical steels. The Mn and S in steels would precipitate as secondary phase in the form of dispersive MnS particles during the production processes and these particles have very important influences on the steel properties. It is generally believed, that the precipitation and coarsening of MnS particles in high grade non-oriented electrical steel could not only reduce obviously the core loss but also weaken the magnetic aging effects during the service time of the steel sheets[4]. The core loss of conventional oriented electrical steels would be reduced by means of high Si content. However, large amounts of dispersive MnS particles as inhibitors are also introduced in conventional oriented electrical steels to control the matrix structure and the abnormal grain growth during the final secondary recrystallization annealing in order to obtain strong Goss texture.

However, due to high Si in such steel (2.7% Si), hot workability is adversely affected. This is reflected in form of elongated structure with high dislocation density. Presence of second phase (austenite), if any, also leads to differential flow leading to cracking thus showing poor workability. In view of this, efforts were made to study such behavior occurring during its processing stages by performing uni-axial compression tests on 2.7% Si steel.

*Corresponding Authors Email : aniketanand@sail-rdcis.com, nkartik@sail-rdcis.com, vkumar@sail-rdcis.com, atul-saxena@sail-rdcis.com

EXPERIMENTAL DETAILS

The chemical composition of material used was ascertained by using Optical Emission Spectroscope (Model-THERMO, ARL 3460) is given in Table 1. The Fe-Si binary phase diagram determined with the help of Thermocalc 3.1® for this composition is shown in Fig. 1.

Table 1 : Composition of the 2.7% Si steel, in wt%

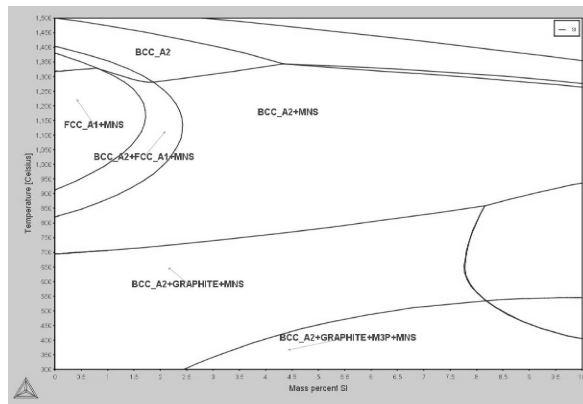| C	Si	Mn	P	S	Al
0.010	2.72	0.054	0.010	0.029	0.011

Fig. 1 : Phase Diagram as determined on ThermoCalc 3.1®

Cylindrical specimens of 15mm height and 10mm diameter were cut from the slab for hot uniaxial compression testing on thermomechanical simulator Gleeble 3500 (Dynamic Systems, Inc.). The hot deformation schematic is shown in Fig. 2. Uniaxial Compression tests were done at temperatures ranging from 1173 K to 1423 K, with a 50 K interval, so as to cover
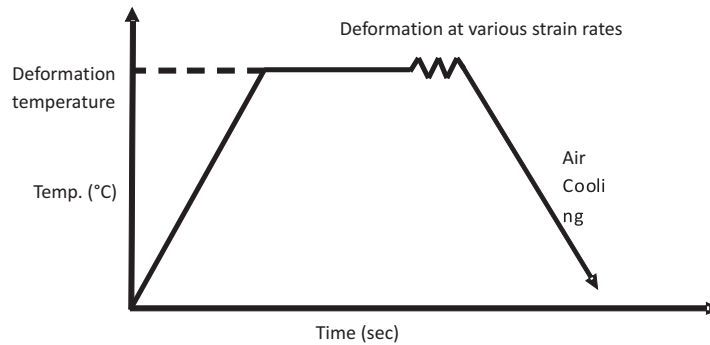

Fig. 2 : Hot Deformation Schematic

the nose of gamma phase (Fig. 1). The strain rates were also varied in multiples of 10 from 0.1/s to 100/s covering the entire processing range. All the samples were heated to deformation temperatures of 1173 K -1423 K for 1 minute and deformed to a total strain of 0.8. After the compression, the samples were air cooled in the test chamber itself. MoS was used as lubricant between the anvil and specimen, and graphite (up to 1273 K)/tantalum foil (>1273 K) of thickness 0.1 mm was used to avoid sticking of the anvil to the specimen surface. Hot deformation software (HDS) was used to run the thermo-mechanical programming in Gleeble 350^{0}C.

After hot deformation, samples were cut in the transverse direction and were copper mounted using hot mounting technique. They were then polished using emery papers and etched using 6% Nital solution for 15 seconds before Microstructural examination under Optical Microscope and Scanning Electron Microscope (SEM).

RESULTS AND DISCUSSION

Flow stress of any material is a function of temperature, strain rate at a particular strain. The general relationship between flow stress and strain rate at constant strain and temperature is represented by Equation 1 [5] :

$$\sigma = C\,(\varepsilon')^{\,m}\big|_{\varepsilon,\,T} \qquad\qquad\qquad ...(1)$$

Where, σ is flow stress, ε is strain, ε' is strain rate, T is temperature and m is strain rate sensitivity. The strain rate sensitivity, m can be determined from the slope of the plot of log σ vs log ε'. It represents thevariation in flow stress with strain rate at particular temperature of deformation. The variation in flow stress is large, the material is said to be strain rate sensitive and it needs to be deformed with great care. On the other hand, if the strain rate sensitivity is small, the material is supposed to be strain rate insensitive and can be deformed with comfort. Uni-axial hot compression test is the most common method to study the flow behavior of material under the influence of temperature and strain rate. Accordingly, tests were carried out to study the influence of deformation conditions (within the broad range of hot rolling of such steels) on flow behavior and ultimately to arrive at the safe rolling window.

The results obtained from uni-axial hot compression test were analyzed and correlated with microstructure examined through optical and scanning electron microscopy.

Effect of Deformation on Microstructure

Microstructural examination of samples deformed at different temperatures and strain rate were carried to study the influence of hot deformation on microstructural evolution, in general, and to identify any softening process, like dynamic recrystallization or recovery occurring during the deformation. This is important in view of the fact that high Si steels are prone to work hardening leading to high rolling load during processing. Optical micrographs of samples deformed at 1223 K and 1423 K and at two different strain rates of 0.1/s and 10/s are shown in Fig. 3. Elongated grains are observed at 1223 K and a strain rate of 0.1/s whereas
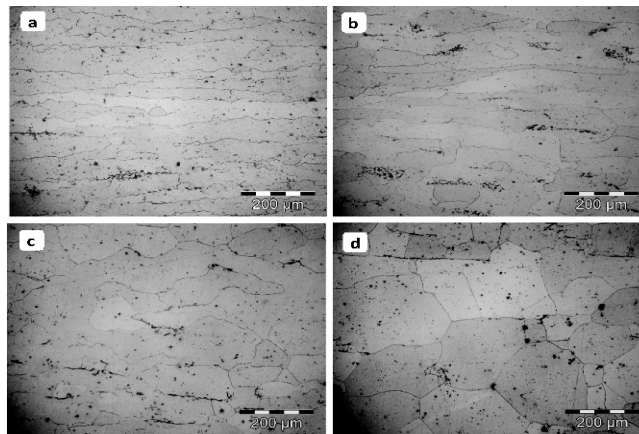

Fig. 3 : Optical Micrographs of Hot-Deformed Samples: a) 1223 K, 0.1/s, b) 1223 K, 10/sec, c) 1423 K, 0.1/s, d) 1423 K, 10/sec

some recovery observed at higher strain rate of 10/s at the same temperature. Extent of dynamic recovery improved with the increase in deformation temperature to 1423 K. At 1423 K, extensive dynamic recovery along with a small amount of recrystallization are observed at a low strain rate of 0.1/s. But, at higher strain rate of 10/s, highly recrystallized equiaxed grains are observed.

Microstructural examination was also carried out with the help of scanning electron microscopy to identify dislocated/ work hardened grains. A typical SEM micrograph in Fig. 4 shows both highly strained and unstrained grains simultaneously reflecting that deformation in
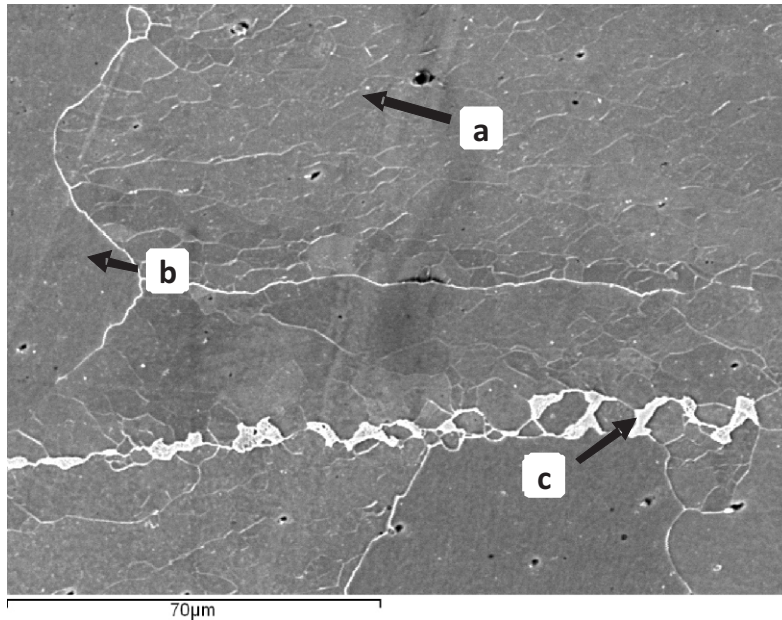

Fig. 4 : SEM Image showing: a) Strained grains, b) Unstrained grains and c) Second-phase

this steel took place preferentially in some grains due to preferred orientation. Presence of sub-grain boundaries in some grains are a good indication of non-recrystallized grain. Further, formation of second phase was observed along ferrite grain boundaries. Elemental analysis confirmed enrichment of C in this phase resembling austenite. It has been reported that presence of more than 0.020 wt% carbon in 3% Si iron passes through a small two-phase a+ g region[6]. The volume fraction of austenite will depend upon amount of carbon present in the steel. In the present steel, it is expected to be about 4% maximum. Since the volume fraction of austenite is very low, it will be present along the prior ferrite grain boundaries. On cooling, the austenite along ferrite grain boundaries will transform to cementite (pearlite) as has been observed and reported.

It is to state that Si steel forms a gamma (austenite) loop. If silicon is low, austenite phase may form as second phase in an otherwise single ferrite phase. Formation of austenite along ferrite grain boundaries will pose problems during processing due to differential deformation and poor hot workability.

Precipitates were also anlyzed to confirm formation of MnS in such steel which is the key to texture development at a later stage of processing. Fig. 5 shows EDAX analysis of precipitate which shows presence of MnS.
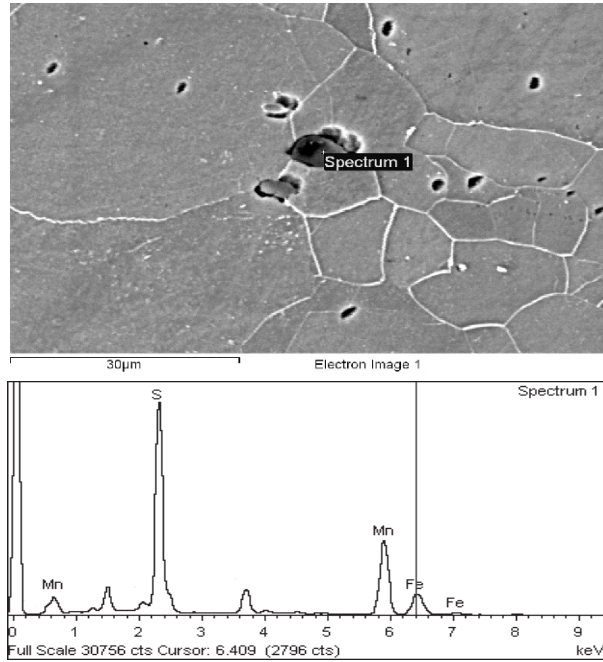
Fig. : 5 EDAX Analysis Showing Presence of MnS Precipitate

Effect of Temperature on Flow Stress

A series of flow stress-strain curves obtained from isothermal compression of 2.7% Si steel at different deformation temperatures at constant strain rates are shown in Fig. 6. It is observed that the flow stress decreases with increasing deformation temperature during the isothermal
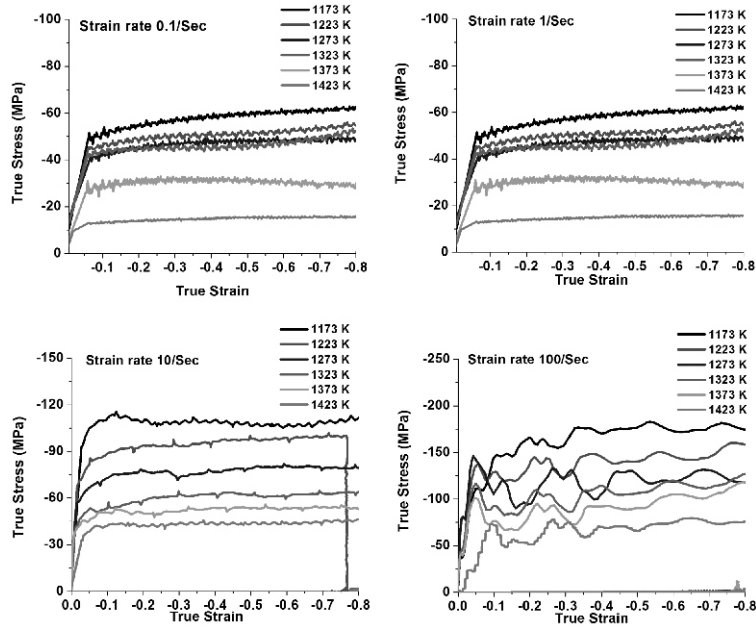

Fig. 6 : Effect of Deformation Temperature on Flow Stress at Different Strain Rates

compression at all strain rates. Dynamic recovery was observed at all temperatures (except 1173 K) when deformed at a strain rate of 0.1/s. At lower temperature of 1173 K, work hardening was observed continuously throughout the deformation with no sign of recovery. Work hardening was also observed at other temperatures of 1223 K through 1323 K towards higher deformation in excess of 0.4 strain. Similar trend in flow behavior was observed when deformed at a strain rate of 1/s also.

However, flow behavior changed at a strain rate of 10/s where we observed serrations in flow stress inthe temperature range of 1223 K to 1373 K. The serrations were of both positive and negative nature alternatively. This may be due to precipitate - dislocation interactions in the presence of MnS precipitate confirmed by EDAX analysis (Fig. 5). However, the actual mechanism for such serrated flow is under investigation. It is to note that there are three mechanisms concerning serrated flow. The first one is the dynamic interaction between solute atoms and dislocations[7]. The second one is larger groups of dislocations move together[8]. The third one is shearing of precipitates by dislocations[9]. Although there is no agreement in the theory of serrated flow, motion of dislocations is necessary condition for it and dislocation - precipitate interaction has a strong possibility in the presence of precipitate, like MnS.

For strain rate of 100/s, we observe continuous work hardening which may be due to very less time available for dynamic recovery.

Effect of Strain Rate on Flow Stress

Fig. 7 shows the effect of strain rate on flow behavior at temperatures of 1223 K and 1423 K. It is observed that as the strain rate increases, flow stress increases owing to enhanced dislocation-dislocation interactions. The optical micrographs in Fig. 3 shows recrystallization
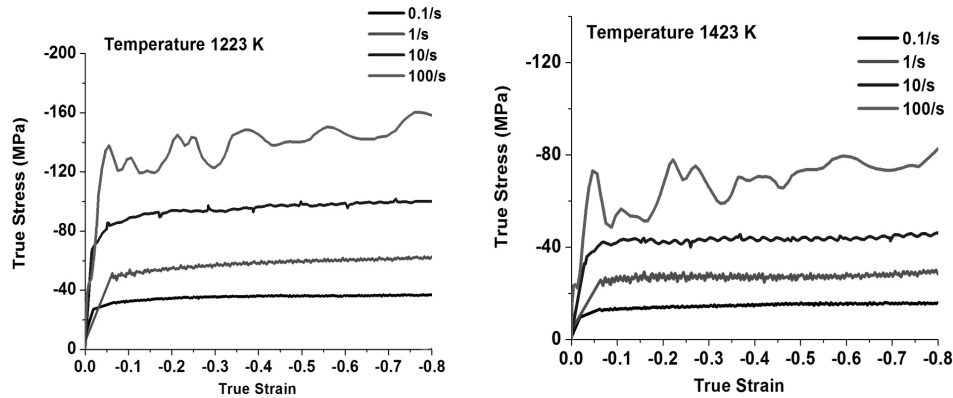

Fig. 7 : Effect of strain rate on flow stress at deformation temperatures of 1223 K and 1423 K

at strain rate of 10/s at 1423 K while at strain rate of 0.1/s only a small amount of recovery is observed . Similarly at 1223 K more recovery was observed at higher strain rate even though the time available for recovery was more at lower strain rates.

Fig. 8 shows effect of temperature on flow stress at a typical strain of 0.4 at different strain rates. It can be observed that flow stress increases with decrease in temperature and with the increase of strain rate. The increase in flow stress is gradual at lower strain rates but becomes steep as strain rate increases with lowering of temperature. This results in increase of rolling load due to which extreme care should be taken during processing of these electrical steels.
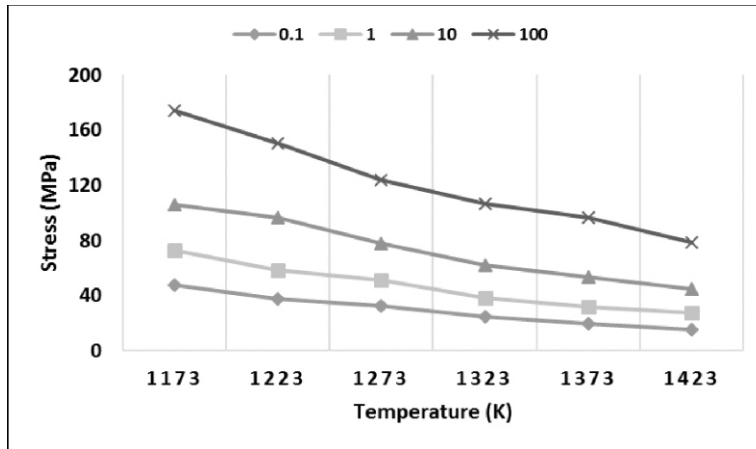
Fig. 8 : Effect of temperature on flow stress at 0.4 strain for all strain rates

Strain Rate Sensitivity

The strain rate sensitivity describes the dynamic material behavior, and is, therefore, an important material property to be determined. The strain rate sensitivity is defined by its relation to the plastic flow curve, and not to the engineering stress-strain curve. Strain-rate sensitivity index is referred to as 'm' and defined as:

$$m = \frac{\delta \log \sigma}{\delta \log \varepsilon'} \quad \text{(At constant temperature and strain)} \qquad ...(2)$$

Where, σ is flow stress and ε' is strain rate[5]. As can be seen in Fig. 9, strain rate sensitivity increases with temperature in general but forms a plateau in the temperature range of 1223 K to 1323 K.
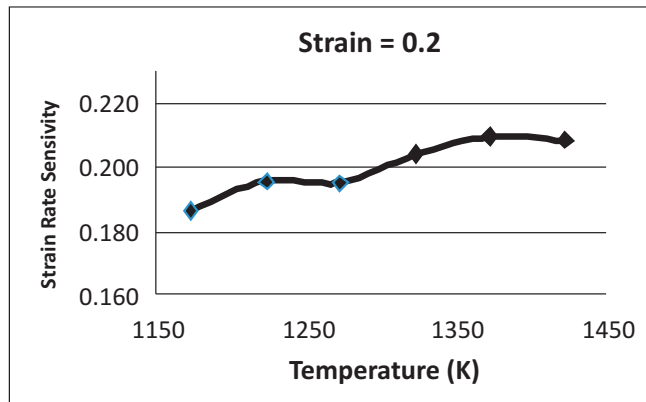

Fig. 9 : Variation of Strain Rate Sensitivity with Temperature

CONCLUSIONS

– Flow stress decreased with an increase in deformation temperature and decrease in strain rate.

– Extent of dynamic recovery increased with increase in deformation temperature and strain rate.

– Recrystallization was observed at 1423 K which increased considerably with increase in strain rate from 0.1/s to 10/s.

– Preferential deformation was observed in some grains due to difference in the orientations of grains.

– Small amount of cementite (pearlite) transformed from austenite along prior ferrite grain was observed due to presence of carbon in excess of 0.02.

– The strain sensitivity of the material increased gradually from 0.19 to 0.21 with an increase in temperature from 1173 K to 1423 K.

REFERENCES

[1] Bertotti G. and Fiorillo F., (1994), Grain-oriented 3 wt%silicon steels. In : Magnetic Alloys for Technical Applications, SoftMagneticAlloys, Invar and Elinvar Alloys, **19**(1), Landolt-Bornstein, Group III Condensed Matter.

[2] Xia Z., Kang Y. and Wang, (2008), Developments in the production of grain oriented electrical steel., *J. Magn. Magn. Mater.*, **320**(20), pp. 3229.

[3] Buschown K.H.J. et. al., ed., (2001), Encyclopedia of Materials: Science and Technology, Elsevier, pp. 4807-4808.

[4] Lyudkovsky G. and Southwick P.D., (1986), the effect of thermomechanical history upon the microstructure and magnetic propertiesof nonoriented silicon steels. Metallurgical Transactions A, **17**A(8), pp. 1267-1275.

[5] George E. Dieter, Mechanical Metallurgy, SI MetricEdn., McGraw-Hill Publishers, London, pp. 297.

[6] Schoen J.W., (1986), High Temperature Grain Growth during Slab Reheating of Oriented 3 Pct Si-Fe Made Using Continuous Casting, Metallurgical Transactions A, **17**A(8), pp.1335.

[7] Sleeswyk A.W., James M.R., Plantinga D.H. and Maathuis W.S.T., (1983), Acta Metall., **31**, pp. 1715.

[8] Korbel A. and Martin P. (1988), Acta Metall., **36**, pp. 2575.

[9] Wang Z.G., Liu W., Xu Y.B., Zhang T.Y. and Zhang Y. (1994), Scripta Metall. Mater., **31**, pp. 1513.